Basis for Coupled 3-D Neutronics and Thermal-Hydraulics

José M. Aragonés

Departamento de Ingeniería Nuclear, Universidad Politécnica de Madrid, 28006 Madrid, España

Abstract. The purpose of this seminar is first to discuss the basis of the coupling between 3-D Neutron-Kinetics and Thermal-Hydraulics codes, including the control and 3-D variables to interchange, the transform of the 3-D NK and TH core nodalizations, and the schemes for temporal coupling and time-step control. As representative examples of the NK-TH core coupling, we discuss first the integration of a 3-D NK nodal code with a TH subchannel code, for detailed transient core analysis; and second the coupling of 3-D NK nodal codes with TH system codes, for general transient and safety analysis. In chapter 2, we analyze several prototype model transients in PWR, where large 3-D core asymmetries are found and the NK-TH coupling is quite significant, including loss-of-flow and symmetric and asymmetric core cooling, considering the effects on the responses of the excore detectors. In chapter 3, we discuss the analysis of an increase-of-flow transient actually occurred in an operating PWR and the comparison with the measured data. In chapter 4, we summarize the phenomena and results of the calculations of the NEA/NSC Benchmark on the main steam line break (MSLB) transient in a PWR. Finally, we will discuss the state-of-the-art issues in LWR coupled NK-TH 3-D transient analysis and ongoing and planned computational developments.

1. BASIS FOR COUPLED 3-D NEUTRONICS AND THERMAL-HYDRAULICS

The purpose of this seminar is first to discuss the basis of the coupling between 3-D Neutron-Kinetics (NK) and Thermal-Hydraulics (TH) codes, including the 3-D variables to interchange, the transform of the 3-D NK and TH core nodalizations, and the schemes for temporal coupling and time-step control. As representative examples of the NK-TH core coupling, we discuss first our Core Dynamics code SIMTRAN for PWR core analysis, which integrates our 3-D NK code SIMULA with the public TH subchannel code COBRA. As a second example we discuss the coupling of our 3-D NK code SIMTRAN with the system code RELAP-5, for general transient and safety analysis.

1.1. Characteristics of SIMTRAN and the coupling of Neutronics and Thermalhydraulics

SIMTRAN is our 3-D PWR core dynamics code [1], under development and validation since more than 10 years [1-15]. It was developed as a single code merge, with data sharing trough standard FORTRAN commons, of our 3-D neutronics nodal code SIMULA and the multi-channel, with cross-flows, thermal-hydraulics code COBRA-IIIC/MIT-2. Both codes solve the 3-D neutronic and TH fields with maximum implicitness, using direct or iterative methods to solve linearized systems.

COBRA-III-C/MIT-2 is a public code [7] for core thermal-hydraulics (TH) calculations, with implicit cross-flows among channels, and homogeneous two-phase fluids. It is used worldwide for TH analysis of the Departure-from-Nucleate-Boiling Ratio (DNBR) in PWR sub-channels, as well as for 3-D whole PWR core simulation with one or more channels per fuel assembly. COBRA uses a direct inversion at each plane of the axial flow equations, with cross-flows updated over an outer iteration loop, for the homogenous model single-phase coolant channels, and a finite-element direct solution of the fuel rod radial temperature equations.

We have refined the COBRA solution methods [7], increasing their implicitness and improving the constitutive relations and solvers, both in the thermal calculation of fuel temperatures and in the implicit calculation of cross-flows. The correlation of the fuel-clad gap conductance has been revised [1], to lower the early fuel-clad contact conduction and to limit its later degradation by release of gas fission products and clad fluence, following integral operating measurements. Early in burnup, it increases with the effective fuel temperature (the same used for Doppler feedback) and local (pellet) burnup; at mid-burnup it increases less with the same fuel temperature and decreases with

the average rod burnup, to a nearly constant value at high burnups. Its calculation is explicit, but the effects of its local change with pellet and rod burnup are noticeable (of the order of 100 degree C). Fuel properties are implicit, requiring very few iterations to converge. The wall-to-fluid heat transfer coefficients are explicit in the fuel temperature calculations and implicit in the cross-flow iterations, but just one iteration is required in most conditions and time-steps, except in transient two-phase regimes, where COBRA homogeneous model is too crude.

SIMTRAN is our coupled code for 3-D dynamic analysis of PWR cores, integrating our NK code SIMULA and the TH code COBRA, following the scheme of figure 1, where the variables exchanged and the external variables driving the transients are shown, together with the correspondence among both NK and TH nodalizations.

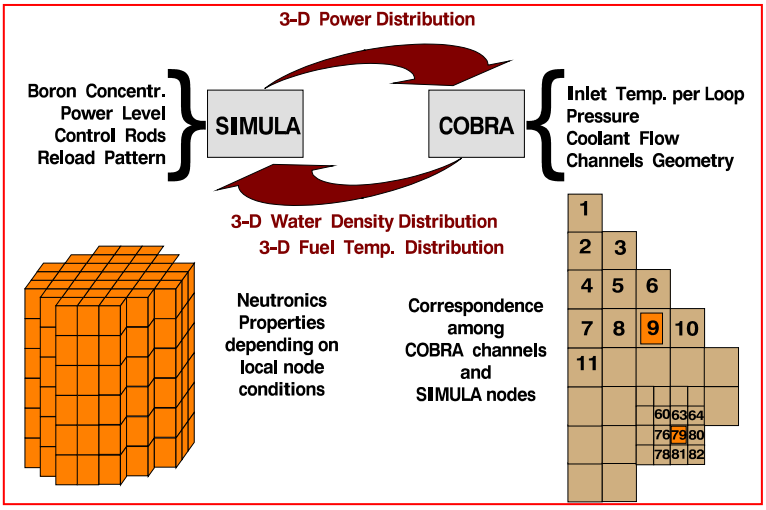

Figure 1. Variables for the 3-D neutronics thermal-hydraulics coupling in SIMTRAN

1.2. Coupled neutron kinetic (NK) and thermalhydraulics (TH) time discretization

In PWR core transients a fully implicit and coupled NK-TH scheme is both cumbersome to implement and to solve efficiently -since the non-linear feedbacks are not amenable to be linearized either analytical or numerically-, while simple explicit schemes require short time-steps, are prone to oscillations and do not conserve energy. The different time-scales of the TH (slow) and NK (fast) phenomena can be exploited by time-splitting techniques.

The 3-D core N-TH coupling is done internally in SIMTRAN by a semi-implicit scheme [1], using a staggered alternate time mesh, as shown in figure 2.

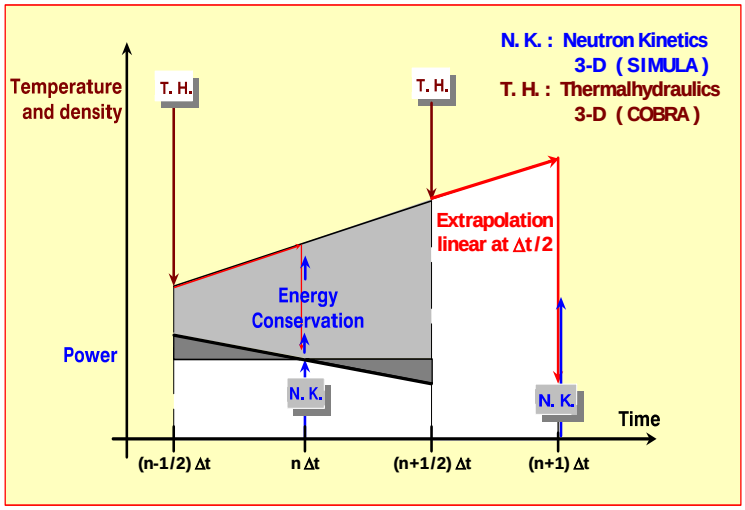

Figure 2. Temporal coupling of N.K. and T.H. for fast transients in SIMTRAN

The TH solution is advanced over one half of the NK time step, thus conserving energy in first order by taking the NK nodal power centered in the time step. Then, the implicitly calculated 3-D TH variables (water density and water and fuel temperatures) are extrapolated over another half of the time step for the NK solution. The neutronics constants are thus nearly implicitly calculated in the next time step as a function of the extrapolated TH variables, where the limited half-step extrapolation prevents of significant oscillations, allowing for larger time steps. The scheme has shown an accurate and robust performance, with minimal diffusion and oscillations [1-15].

This scheme is also rather easily implemented in a modular way, requiring an interfacing routine for mesh transformation, exchange of variables -via commons for efficiency- and time-step control. Since the extrapolated densities and temperatures for the NK module are stored in different variables as in the TH module, which saves also those at the previous time-step, the accuracy of the half-step extrapolation is tested in the next time-step, providing simple criteria for its reduction -with shorter extrapolation- or increase -progressive to limit the extrapolation error-.

1.3. Special TH models: Mixing of flow from loops in the vessel and subchannel analysis

We have integrated, optimized and validated in the SIMTRAN code these special thermalhydraulics models. The core channels, coupled through implicit cross-flows, have been extended up to the thermocouple locations, above the fuel assembly top head/nozzles [1]. Three unheated axial nodes have been added to each channel, with different equivalent channel characteristics and heights, to model the sections with "empty" fuel rods (plenum) and the top grid, the "gap" space to the top assembly heads, and the head/nozzle region. The additional cross-flow mixing in these extra top nodes redistributes the water temperatures at the thermocouple locations up to 1 ºC.

In reactors with multiple loops it is of special interest to model the water flow and enthalpy mixing from the cold legs inside the reactor vessel (*downcomer* and bypass) up to the inlet of the core channels (figure 3), as well as the mixing from the outlet of the core channels in the upper plenum up to the hot leg nozzles. The effect of enthalpy mixing is quite important for realistic analysis of asymmetric core transients with cooling of a single cold loop, such as the steam-line break, or with Boron dilution also in a single loop.

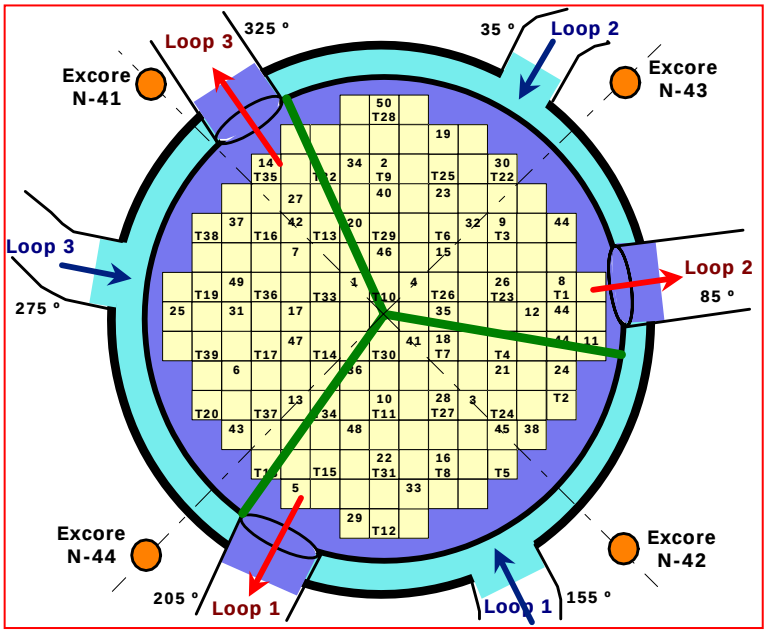

Figure 3. Mixing of flow-enthalpy from loops and effect in the excore detectors

SIMTRAN incorporates an empirical model of the mixing among the cold leg inlets to the vessel to yield the enthalpies at the inlets of the core channels [6,12,15]. The model uses Fermi functions for the inlet channel enthalpies in terms of the products enthalpy-mass flow-distance between the vessel inlet of each loop to the core channel inlet, with a single parameter to be fitted to the measurements. The model allows for extreme mass flow and enthalpy variations per loop, as well as for rotational mixing. The same functional model is used too for the mixing from the outlets of the core channels to the vessel outlet nozzles of the hot legs, with a different mixing (exponential) parameter, with larger mixing in the hot upper plenum.

Another special effect to model is that due to the changes in the loop inlet temperatures (cold legs), that cause changes in the water density of the core reflector (*downcomer* and bypass) and hence in the exponential attenuation of the neutrons that leak from the core through the vessel internals and wall, thus causing the variation of the currents at the excore detectors. SIMTRAN uses general response matrices, with exponential attenuation in the reflectors proportional to the water density changes, with each detector affected by the different inlet cold legs, to account for this effect [2,3,6].

Other capability developed in SIMTRAN [1,17] is to perform detailed DNBR analysis in the hottest core sub-channels, using 3-D and pin-by-pin powers, by offline COBRA calculations in one or more sub-domains, with a detailed adaptive mesh, as sketched in figure 4.

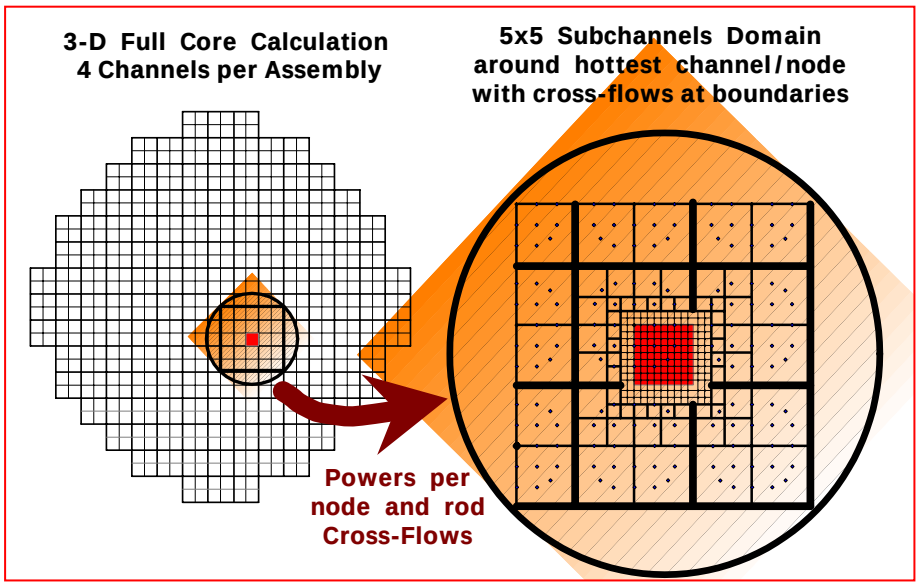

Figure 4. Analysis of the DNBR per sub-channels in sub-domains with adaptive mesh

The embedded subchannel analysis has been developed as an offline COBRA calculation of a part of the core, using the whole core SIMTRAN solution, with nodes/channels per quarter of assembly, to select the worst channels and to provide the power distributions and boundary cross-flow conditions. The worst channels are selected by the product of peak pin to node average power ratio by the maximum clad temperature in the equivalent channel. The pin powers inside the worst and surrounding nodes are reconstructed from the COBAYA pin-by-pin power database and the 3-D nodal power. The subchannel geometry includes each individual fuel pin or water/absorber tube and associated subchannels inside the worst node/channel, and progressively lumps rods/subchannels in the surrounding ones, with a maximum of 2 to 1 interconnections, up to the next row of full size node/channels or the core support plate. At the outer boundary, the cross-flows from the whole core solution are imposed. An auxiliary code performs all the geometry, power and boundary data preparation for the automated COBRA subchannel calculations. This procedure provides the detailed best-estimate thermal margins, as well as the checking of the SIMTRAN average channel models [1,17].

1.4. Coupling of SIMTRAN to RELAP-5 and TRAC-M

In the frame of the project for a *consolidated T/H code* of the US-NRC, Prof. T. Downar and his group at the University of Purdue have developed and distributed [20-21] a “General Interface” to couple the 3-D neutronic code PARCS to the TH system codes RELAP5 and TRAC-M.

Sets of similar routines have been implemented in these codes to perform the data transformations between the different meshes (“*Data Mapping*”) of the respective codes, with their own dispositions in memory. This is done by using “vectors”, that group all the data to be exchanged, and are transmitted among the codes via standard PVM (*Parallel Virtual Machine*) library, developed at ORNL by J. Dongarra. An intermediate program (GI) “gets” these vectors, as well as the semaphores of communication and error, “multiply” them by the permutation matrices for the mesh transformation, and “sends” the product vectors to the other code, also via calls to PVM routines. Figure 5 shows this coupling scheme.

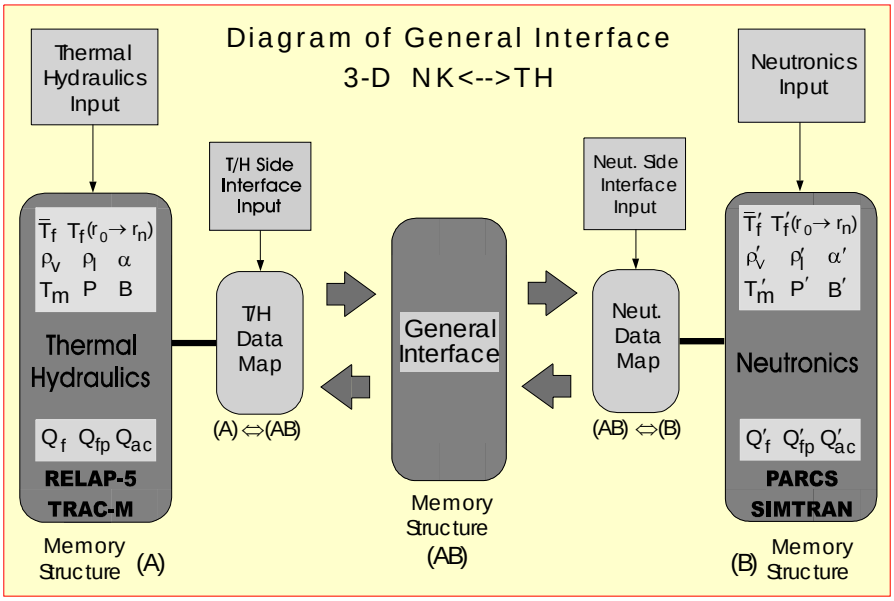

Figure 5. Scheme of the coupling between PARCS or SIMTRAN and RELAP-5 or TRAC-M

This coupling scheme was designed and implemented with emphasis in the maximum flexibility and minimum modifications in the existing codes, to facilitate their maintenance and portability to other neutronics and thermal-hydraulics codes. For its implementation in our SIMTRAN code [12,15], we have adapted the set of routines PDMR that perform the "mapping" of the data to transmit and acquire, to or from the memory layout of PARCS or SIMTRAN and the exchange vectors, and the calls to PVM routines, just replacing the data in the PARCS memory layout (commons) by the corresponding data in the SIMTRAN commons, by a direct mesh transform among both 3-D nodal meshes. In this way the permutation matrices for the general interface (GI) are just the same ones generated to couple PARCS with RELAP-5 or TRAC-M, simplifying the management of the data bases for validation and applications.

In the implementation in SIMTRAN we have used our semi-implicit scheme for time coupling in a staggered mesh, described in 1.2 and figure 2 above. In the present version [12,15], all the COBRA routines have been suppressed, acquiring all the TH variables from the system code.

In the present versions of RELAP-5 y TRAC-M the number of hydraulic channels parallel or coupled in the core and reflectors is limited, to 18 and 1 respectively in practical nodalizations, while the number of heat structures that can be used is much larger, with one mean fuel rod for each fuel assembly. In future work we plan to reinsert the COBRA code for a more detailed TH core modelization, with one mean channel and fuel rod per assembly or quarter of assembly, using consistently the TH variables at core inlet and outlet.

2. ANALYSIS OF 3-D PROTOTYPE MODEL TRANSIENTS IN PWR CORES

In this chapter we analyze several prototype model transients in PWR cores with a single cause, only a single core inlet or control variable is changed, without any external feedback on other variables from the full system response, and without control scram (like in ATWS). We consider transients with a significant redistribution of the incore neutron flux and power (axial or radial or both) to test and analyze the 3-D incore NK-TH coupling and feedback. The transients are calculated with our SIMTRAN code for an operating reactor (Vandellós II, W-PWR) [6,11].

2.1. Model Loss of Flow transients without scram at BOC-HFP

We consider two classes of loss-of-flow transients in PWR cores: the slow *coast-down* (LOF), in 30 s, and the sudden *rotor-block*, en 1 s, in both cases of a single primary pump (in a 3 loop reactor). The analysis is done at the worst initial conditions: at beginning of cycle (BOC) and nominal power without xenon (HFP), when the boron concentration is higher and, hence, the moderator temperature coefficient (MTC) is less negative, then the reactivity loss is minimal and so is the power level decrease, worsening the thermal margins.

In the slow coast-down of flow in one loop (out of 3 loops), the total flow through the core slowly decreases to 66.6 % of the nominal flow in 30 seconds. In the rotor block, the core flow goes to that value suddenly, in just 1 second. Figure 6 (left) plots the coast-down with time of the total core flow and the flows at the affected loop and at the two intact loops. All other core conditions (nominal) are kept constant. Figure 6 (right) plots the calculated core power evolution.

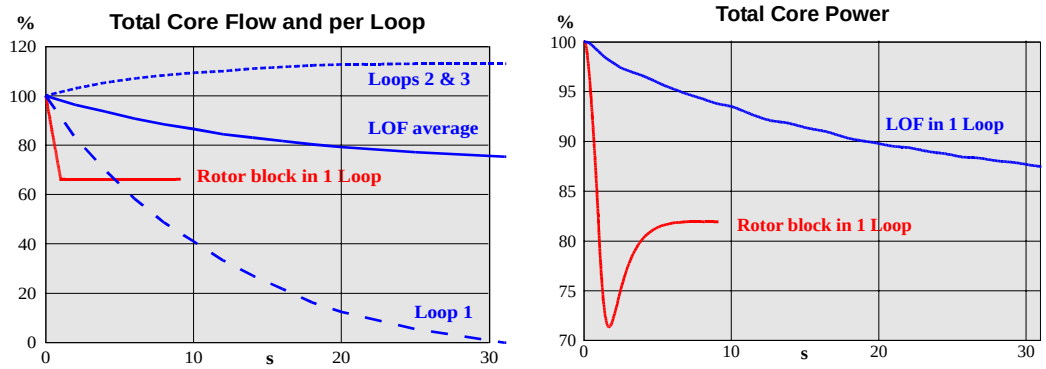

Figure 6. Coolant flows (left): core average and per loop and core power (right) for a single pump coast-down and rotor block loss of flow transients

In the slow loss of flow by coast-down of a single loop pump, the total core power slowly decreases to 87 % of nominal power in 30 seconds. In the sudden rotor-block of a single loop pump the core power quickly goes down to 71 % of nominal power at 2 seconds and then goes quickly up, stabilizing to 82 % at 6 seconds.

Figure 7 plots the evolution of the maximum clad and coolant temperatures (at left) and the calculated minimum DNBR (at right), the ratio of the critical heat flux for departure from nuclear boiling to the maximum local heat flux, where the first is calculated using the open Westinghose W-3 correlation. The increase in the maximum clad temperature is very small, reached at 2 seconds with an increase of 12 degrees C. The maximum coolant temperature, at the outlet of the hottest channel, reaches the saturation temperature very quickly, also at 2 seconds, in the sudden rotor-block transient. In the slow coast-down loss of flow of a single pump all maximum temperatures increase very little and very slowly, and the DNBR decreases very little.

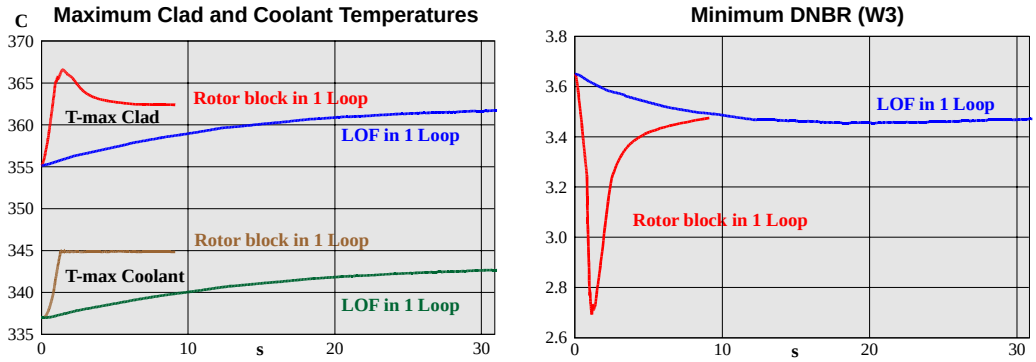

Figure 7. Maximum clad and coolant temperatures and minimum DNBR in loss of flow transients

In the rotor-block sudden loss of flow transient the power redistribution is very significant, with power reduced in the top (hottest part) of the core, in addition to the power level decrease, so that even with the water reaching the saturation temperature in many channels, with voids up to 22 %, the DNBR is well above its limit (1.40 with the W-3 correlation).

2.2. Model Core-Inlet Water Cooling Transients without scram at EOC-HFP

We consider very fast water cooling transients in one or all of the reactor loops, without scram and in the worst initial core conditions: no Boron, at end-of-cycle (EOC), rated power (HFP) with equilibrium xenon, and all-rods-out (ARO); when the moderator temperature coefficient (MTC) is more negative, thus resulting in the highest reactivity and power increase.

The inlet water cooling considered are of -10 and -15 degrees C in all 3 loops, and -30 y -45 degrees C in a

single loop, at constant cooling rate during 1 second, resulting in equal decrease of the average core inlet temperature. The enthalpy-flow mixing of the 3 cold leg flows at the in-vessel down-comer and lower plenum is performed as described in §1.3, with the exponential factor of the Fermi functions fitted to the experimental measurements: 10% and 20% mixing in the lower and upper plenum, respectively. The SIMTRAN results are shown in figures 8 and 9.

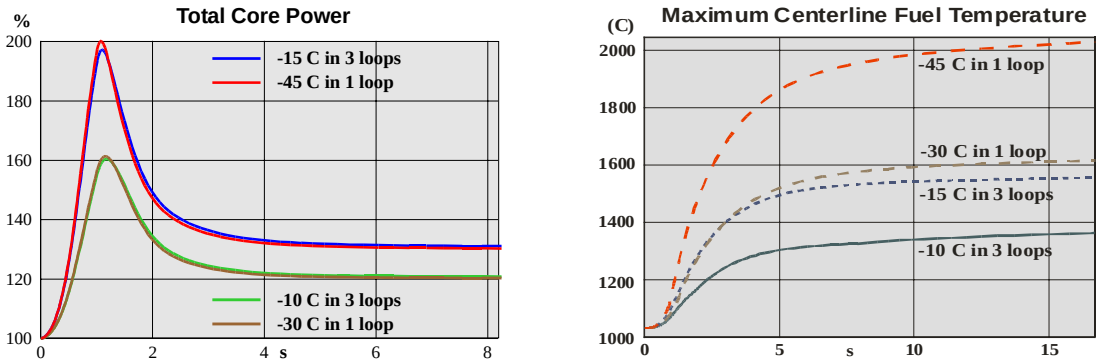

Figure 8. Total core power (left) and maximum centreline fuel temperature (right) in model transients with core-inlet water cooling in 1 and 3 loops, at EOC-HFP-Eq.Xe-ARO.

In the asymmetric cases, with cooling of a single loop, there are not significant differences in the evolution of the total core power, but there are big differences in the maximum coolant and fuel temperatures, because the power increases specially in the part of the core affected by the cooling of the single loop, while the power increases symmetrically in the uniform cooling of the 3 loops.

The core power quickly grows up to 160% and 200% in 1 second, just at the end of the cooling time, decreasing afterwards towards the asymptotic levels of 120 y 130 %. The maximum centreline fuel temperature increases with the energy deposited by the peak of power, up to rather high values in the inlet water cooling of a single loop.

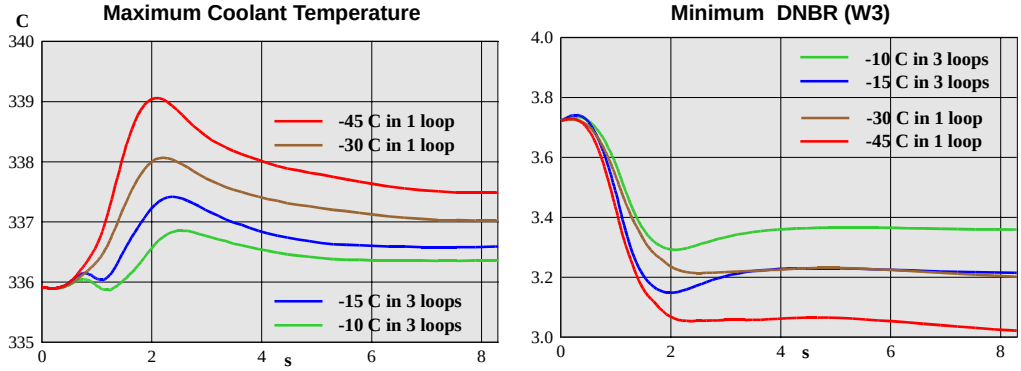

Figure 9. Maximum coolant temperature and minimum DNBR in inlet cooling transients in 1 and 3 loops

The maximum coolant temperature increases, but only 2 or 3 degrees C, up to a peak at 2 seconds (1 s of cooling time plus 1 s of core pass time), decreasing afterwards to very small increments. Both variables show a different evolution in asymmetric cooling transients.

To gain more insight in the interdependency of the distributions of the local power and the local coolant temperature, we show in the following the results of a more simple prototype transient, with a cooling of a single loop of -20 deg-C and a heating of the other 2 loops of +10 deg-C, without changing the average core inlet temperature nor, hence, the total core power.

Figure 10 shows the coolant temperatures at the inlet of the fuel channels, after the in-vessel mixing in the down-comer and lower plenum. The zone of mixing is relatively narrow and equidistant of the inlet nozzles of the cold legs to the reactor vessel. Figure 11 shows the change, relative to the initial, of the fuel assembly powers at 2 seconds of the transient with asymmetric cooling-heating of the inlet loops, when the power redistribution is maximal.

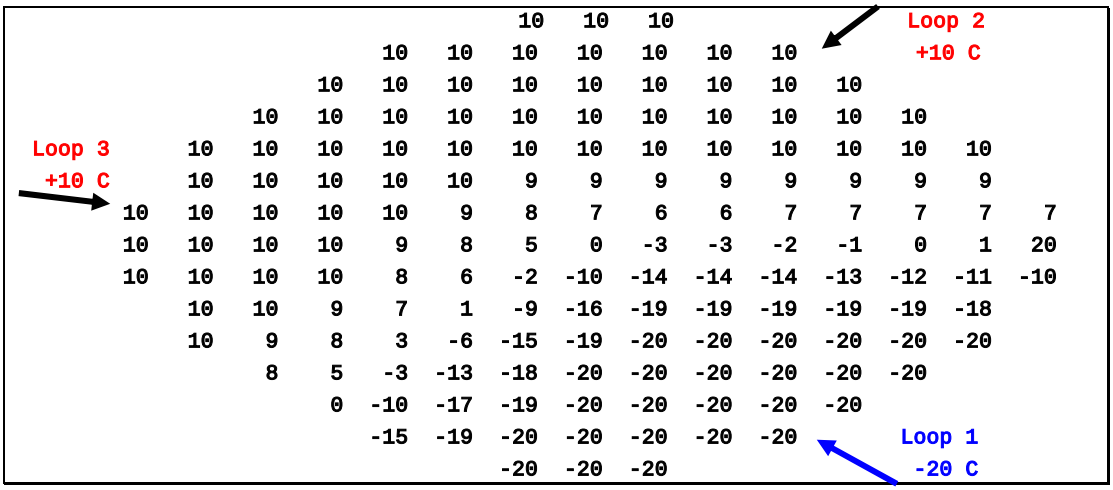

Figure 10. Differences (deg-C) in the inlet water temperatures per loop and channel (at lower plenum)

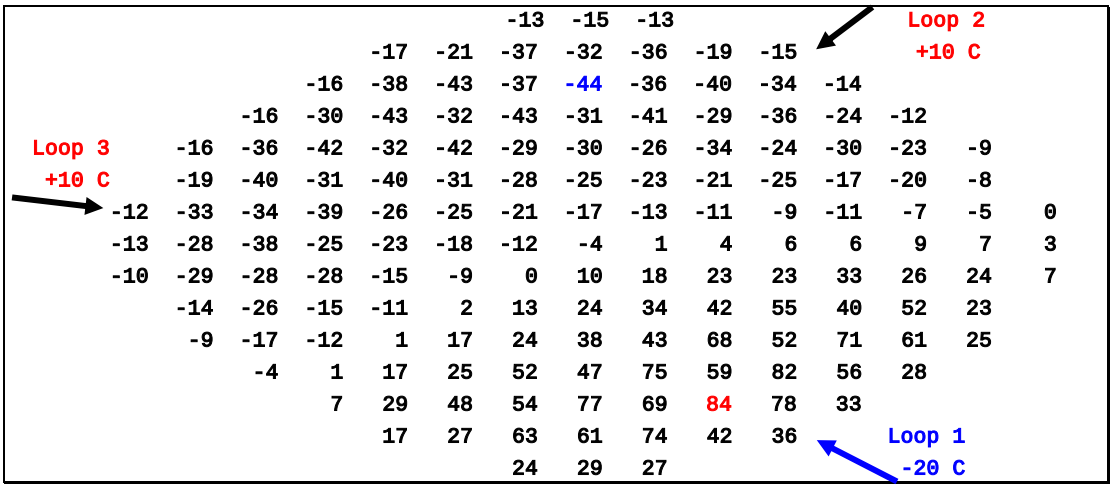

Figure 11. Change (%) of the relative fuel assembly powers at 2 s of the asymmetric cooling-heating transient

The power redistribution is rather large and symmetrical, in half core with reference to the axis parallel to the inlet nozzle of loop 1. The larger power increases, up to 84%, show in the core zone closer to the inlet of the cooled loop 1, while power decreases, up to -44%, in the core zones closer to the hotter loops 2 and 3. Figure 12 shows the change in the core outlet coolant temperatures.

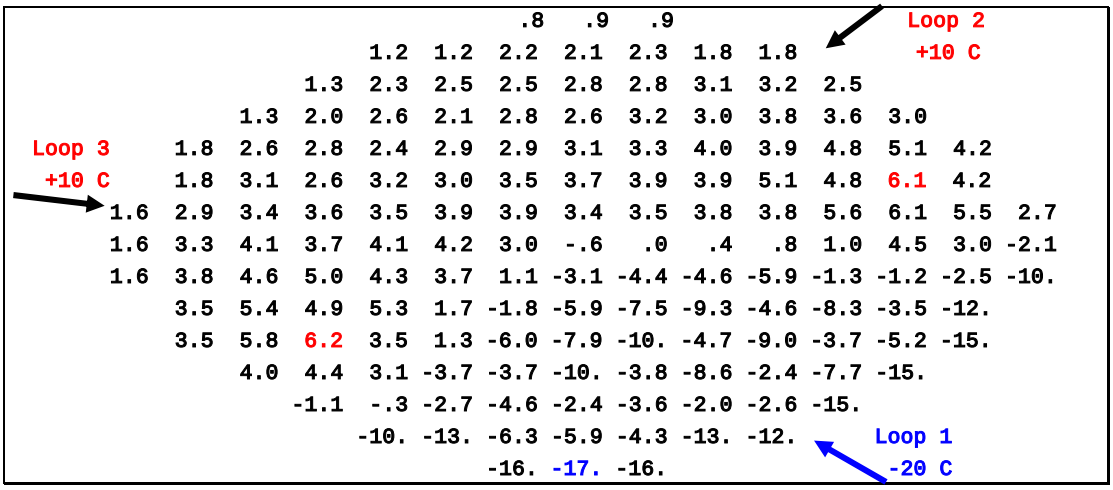

Figure 12. Change (deg-C) in core outlet temperatures at 2 s of the asymmetric cooling-heating transient

The coolant temperatures at the core outlet of each fuel assembly channel decrease in the core zone close to the inlet of loop 1, which is just the zone with lower coolant inlet temperatures but higher power. The coolant outlet temperatures only increase, and very slightly, in the core zone of mixing of the core inlet temperatures, because the neutron diffusion produces a power increase in that uncooled zone by the proximity of the cooled-down core zone, with higher neutron flux, close to loop 1 inlet.

Figure 13 shows the effect of the asymmetric cooling of the inlet water at the radial core reflector (downcomer) and in the responses of the excore detectors, as calculated by SIMTRAN.

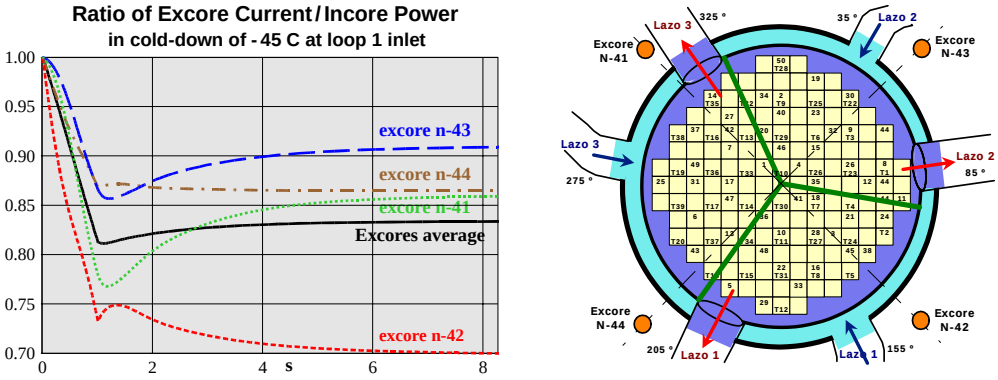

Figure 13. Ratio of the excore powers, obtained from the measured currents at the 4 excore detectors, and the incore power in asymmetric inlet water cooling transients

The ratio among the normalized *excore* powers to the *incore* power decreases, on average a 12 to 13 %, when the inlet of a single loop is cooled down -40 deg-C. In the excore detectors located far from the inlet nozzle of the cooler loop 1, because they receive less neutrons from their closer core zones where the power has decreased. In the excore detectors close to loop 1, because the increase of the density of the cooler water in the reflector (*downcomer)* increases the neutron attenuation of the neutrons produce in the core zones with larger power.

2.3. Effect of symmetric and asymmetric inlet water cooling on Shutdown Margin

Figure 14 shows the calculated shutdown margin (keff-1) for a PWR core, with all control rods fully inserted, but one rod, stuck out in the worst core octant at 0 ppm, EOC (worst MTC), HZP, symmetric (1 loop) and asymmetric (all 3 loops) inlet water cooling with equal average core inlet water cooling.

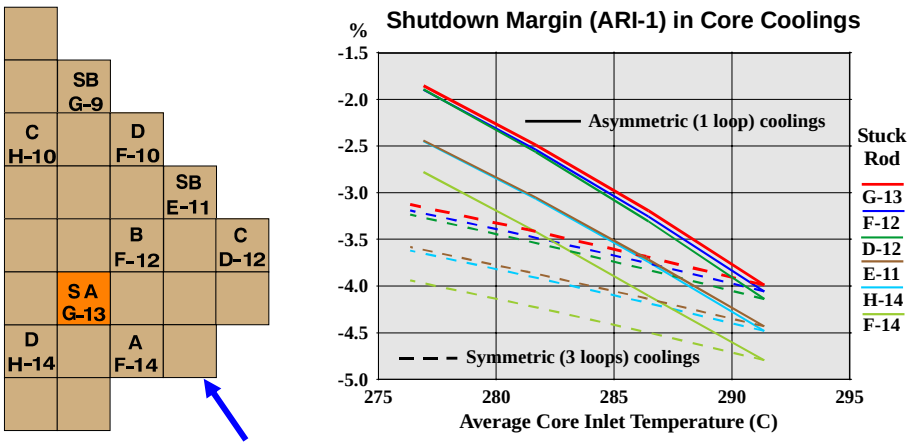

Figure 14. Shutdown Margin (%) in core inlet water cooling in 1 and 3 loops

The Shutdown Margin is significantly reduced for asymmetric cooling in one single loop. The worst stuck-out control rod is the same (G-13) for inlet water cooling in 1 or 3 loops with equal core average inlet water cooling.

2.4. Conclusions of the analysis of prototype model transients in PWR cores

The scope of the SIMTRAN capabilities in 3-D PWR core fast transients has been showed, with the following main conclusions [6-11]:

- Transients of loss of flow without scram:
  - Mitigated by the axial redistribution of power.
- Transients of fast inlet water cooling:
  - Mitigated by the in-vessel inlet water mixing and by the 3-D power redistribution in asymmetric cooling of a single loop.
  - Worsened by the reduction in the excore detector response (not conservative).
  - Reduced Shutdown Margin of ARI-1 condition for asymmetric inlet water cooling.

In general, we obtain significant 3-D redistributions of power and temperatures in most of these model transients, demonstrating the need of 3-D coupled core neutronics and thermal-hydraulics codes for realistic and detailed transient analysis.

3. ANALYSIS OF A FLOW INCREASE TRANSIENT IN AN OPERATING PWR

We analyze an actual transient of fast core flow increase that occurred in an operating PWR, Vandellós-II in December 1991. First, the transient will be described and characterized and, then, the results of the calculations by SIMTRAN will be shown and compared with the measured data [1].

3.1. Phenomenology, measurements and characterization of the transient

The chain of events that occurred in this actual core flow increase transient was:

(1) A bolt strikes the external electric net connected to the power plant
(2) The electrical protections open. Power plant in electrical island
(3) The generator speeds up due to the loss of electrical load
(4) The internal electrical frequency increases 7 % in 1 second (signal X6506 below)
(5) The primary pumps speed up and increase the core flow (signal F0400)
(6) The water cools down at core passing and the core power increases to 106 % of initial nominal
(7) The excore detectors (signal N0049) trigger the core trip flux-increase setpoint (>5 % in 1 s)
(8) The control rods scram and the turbina trips.

The measured signals, registered by the process computer every 20 miliseconds, were:

- Electrical frequency (X6506)
- Flows at hot legs of loops (F0400)
- Excore nuclear power, from sum of excore currents (N0049)
- Incore Axial-Offset of power, from differences of excore currents (N0041-N0042).

The time evolution of the core flow was inferred with a delay from the time evolutions of the electrical frequency, due to the pumps inertia, but in advanced of the measured flows at the hot legs of each loop (3 loops), because of the delay of the flowmeters (in a bypass of the hot legs) and their time of scrutiny.

From the analysis of the signals of the 3 flowmeters in each of the hot legs, and the currents of the 4 excore detector columns, we concluded that the evolution was symmetrical in all of the 3 loops, both in flows and temperatures. It was also symmetrical in the 4 columns of excore detectors, with similar increases in the sums (neutronic power) and differences (axial-offset) of the measured currents during the power increase and the scram, which indicates that there was not a radial redistribution of power. The assumed core flow evolution is shown in figure 15 (left), in between the registered signals of the frequency and the flow at hot legs.

The control rod scram curve, rod insertion versus time, is also shown in figure 15 (right). The scram is assumed to be initiated at 1.2 seconds of the transient, by the set-point of high increase rate of the neutron flux. The fall of the control rods is assumed to be simultaneous with three stages: constant acceleration by gravity, constant speed by viscous fluid limits and deceleration at the dashpot zone of the guide tubes, that acts as a hydraulic brake. The times of each stage have been fitted to the averaged fall times of the control rods measured at the beginning of that cycle:

1.7 seconds from top to the dashpot and 0.5 seconds to stop.

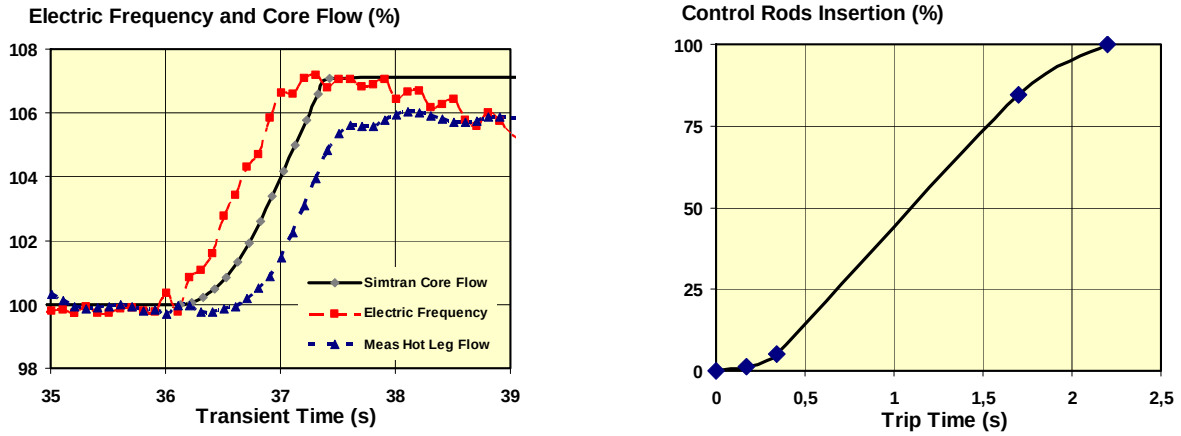

Figure 15. Time evolution of electric frequency and core inlet flow and control rod scram curve

3.2. Results of the SIMTRAN calculations and measurements

The evolution of the core power and its axial offset, calculated and measured, is shown in figure 16.

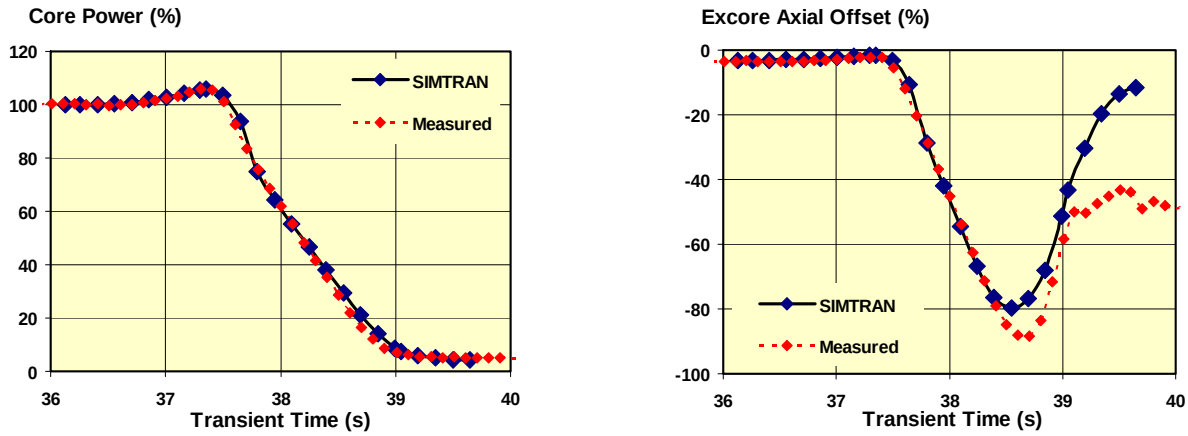

Figure 16. Nuclear power (left) and axial offset (right) calculated by SIMTRAN and measured

The core power increases from the 100% nominal value, at the initial time of the transient, up to 104% at 1.2 seconds after the flow increase, when the control rods trip, with a quite good agreement with the measurements. The axial offset of core power also shows a moderate increase, also up to rod trip, due to the added reactivity at the top of the core by the reduced water heating with the flow increase. This is seen more clearly in figure 17 (left), where the axial core power distributions are shown at the initial time of the transient and at the time of maximal power.

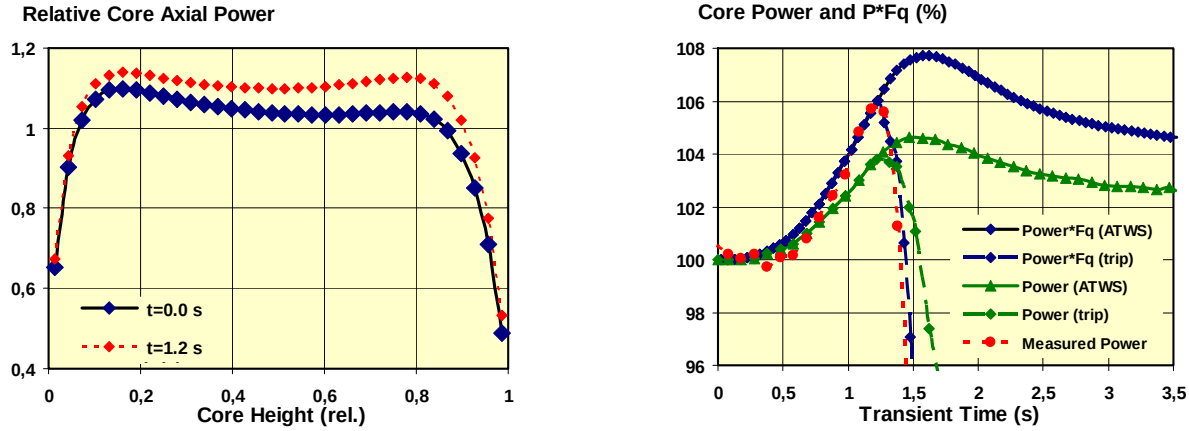

Figure 17. Axial core power distribution at t=0.0 s and t=1.2 s and total core power and peak

relative power in transients with and without scram.

Since the trip setpoint of high flux change rate is not of safety class, it is of relevant interest to calculate the transient without scram, whose results are shown in figure 17 (right), compared with the calculated and measured core power evolutions with scram, also drawn in zoomed scale in this figure. At the top of this figure we also show the calculated maximal relative local power, at the hottest fuel pellet, it is the relative power (%) multiplied by the local peaking factor F_q, for both cases: with and without scram.

We can see how the actual scram terminated the power increase before its maximum. Without scram the power would had grown to 104.5%, instead of up to 104%, and the maximal local power up to below 108%, instead of up to 106%. It is, the Doppler would have limited the power peak just at 1.6 seconds of the transient, instead of at 1.2 seconds with the scram.

3.3. Simplified analysis using the nominal core average reactivity coefficients

The simplified analysis, similar to point kinetics, is done in terms of the core average reactivity coefficients, calculated at nominal conditions, with the balance equations of power P versus flow Q and coolant temperature difference ΔT and the reactivity balance equations at the initial and final conditions:

$$P_0 = C_p^M \; Q_0 \; \Delta T_0 \qquad \textit{(Initial power balance)} \tag{1}$$

$$P' = C_p^M \; Q' \; \Delta T' \qquad \textit{(Final power balance)} \tag{2}$$

$$\alpha_{T_M} \Delta T_M + \alpha_{P_D} \Delta P = 0 \qquad \textit{(Reactivity balance)} \tag{3}$$

The measured conditions of core power, coolant temperature increase and relative water flow change, with the reactivity coefficients calculated by SIMTRAN in the design analysis at nominal conditions, are the following:

$$P_0 = 100\% \;\; ; \;\; \alpha_{P_D} = -8.04\, pcm/\% \;\; ; \;\; \Delta T_0 = 35^{\circ} C \tag{4}$$

$$\frac{\Delta Q}{Q} = 7\% \;\; ; \;\; \alpha_{T_M} = -45.72\, pcm/^{\circ} C \tag{5}$$

With these data and equations (1) to (3), the power increase from the initial to the final state is calculated as:

$$\Delta P = \frac{\dfrac{\Delta Q}{Q_0}}{\dfrac{1}{P_0} + \dfrac{2\,\alpha_{P_D}}{\alpha_{T_M}} \dfrac{1}{\Delta T_0} \left(1 + \dfrac{\Delta Q}{Q_0} \right)} \approx 3.4\,\% \tag{6}$$

The appearance of a maximum in the power evolution is due to the existence of a delay in the fuel heating: the fuel temperature increase (ΔT_f) can be expressed as:

$$\Delta T_f = \frac{1}{C_p \, M_f} \int \Delta P(t)\, dt \tag{7}$$

where two factors intervene: $C_p \; M_f$, the fuel thermal capacity multiplied by the core fuel mass, and the integral $\int \Delta P(t) dt$, that is the power increase integrated with time, it is the additional energy deposited in the fuel. After the maximum, the increase in core power (at constant flow Q', without scram) tends to 4 %.

3.4. Analysis of alternative transients: inlet water cooling and flow increase at other burnups

To analyze the difference between the transients caused by core flow increases and by inlet water coolings, with the same decrease of the core average coolant temperature, the results of these cases are shown in figure 18 (left) for the transients without scram, where the flow increase results are the previous ones and the core average coolant temperature drop is calculated with equations (1) to (6) above. While the peak in total core power is near the same for both cases (103.4% and 104.1%), the local peak power ($P.F_q$) is just below 106% for the inlet water cooling transient, lower than just below 108% for the flow increase transient, because the last one causes a significant axial power

redistribution while the first one, with a quasi uniform coolant temperature cooling, maintains the initial axial power distribution.

Finally, we have analyzed the same flow increase transient (7% in 1 s, from nominal state) at several cycle burnups, including beginning-of-cycle (BOC) at HFP-ARO with equilibrium xenon, the cycle burnup of the actual transient (7.74 GWd/t) and at end-of-cycle (EOC) at about 10.5 GWd/t for this one-year cycle. The initial steady-state is at nominal conditions HFP-ARO-Eq.Xe and with the critical boron concentration. The results for these 3 transients without scram are shown in figure 18 (right), where the evolution of the local peak power ($P.F_q$) along the transient is compared at these 3 different cycle burnups.

We see that the local peak power shows a higher maximum at higher cycle burnups, due not only to the more negative moderator temperature coefficient (MTC) as boron is diluted with cycle burnup, but also to the higher neutron importance of the top part of the core due to the higher accumulation of plutonium by the increase in ^{238}U resonance neutron captures with lower coolant density. In a flow increase transient the water cools down near linearly, from 0 at the core bottom to its maximum at the core top.

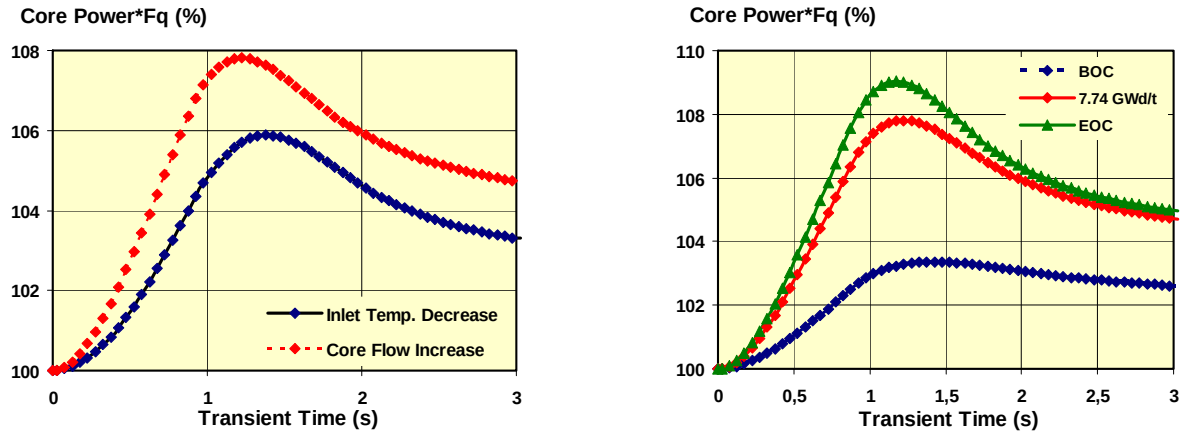

Figure 18. Evolution of local power in transients by ΔQ and ΔT_{inlet}, with equal decrease of the core average temperature (left) and by equal flow decrease at different cycle burnups (right).

3.5. Conclusions of the analysis of the flow increase transient

- The simulation reproduces quite well the measurements: evolution of the nuclear core power and the incore axial-offset as calibrated from the excore detector currents.
- If the control rod scram had not actuated the core power and the peak local power, as given by the product $P \cdot F_Q$, would had been well below the design margins for overpowers.
- The simplified analysis, with balances of power versus flow and temperature jump and with reactivity coefficients, does not yield the observed power increase, nor the calculated local power peak.
- The full transient, 3.5 seconds of real time, is simulated with time steps of 0.05 s, now in less than 3 seconds of computing time using a Pentium-4 processor at 3 GHz.

4. ANALYSIS OF ROD DROP AND GROUP INSERTION TRANSIENTS IN OPERATING PWRS

We analyze two actual transients, a single control rod drop and a fast insertion of a control group (4 rods), which occurred in two operating PWR: Ascó-I in cycle 17 on 9 September 2003 and Vandellós-II in cycle 16 on 2 December 2007, respectively. First, the transients will be described and characterized and, then, the results of the calculations by SIMTRAN will be shown and compared with the available measured data.

4.1. Phenomenology, measurements and simulation of the single control rod drop transient

The chain of events that occurred in this actual single control rod drop transient was:

(1) At 03:02 on 09-sep-2003 a single control rod (E5) drops unexpectedly due to an electronic failure in the rod drive system. Core was in nominal state at 3624 hours (5996 MWd/t) in cycle 17, at 100% power (2940 MWt) with all rods out and 1424 ppm measured Boron.

(2) Power drops in 2.5 seconds to a minimum of 88% and then increases to a stable level of 94% at 10 seconds

after the rod drop. Coolant temperatures at vessel outlet and inlet cool-down asymmetrically by loop.

(3) The operators realize the rod drop event, by the high quadrant tilt observed (about 6%), and following the Tech-Specs start the control bank insertion and Boron addition to lower the power to 66% in about 2:30 hours after the rod drop. At 07:20, about 4 hours after the rod drop, they initiate a slow manual extraction of the dropped rod, completed at 08:30.

Figure 19 shows the SIMTRAN calculated results for the power and quadrant tilt evolution in this rod drop transient. Measured data were only available at 1 minute intervals and good agreement was obtained at that time scales. The safety margins on DNBR and Fq were assessed and found to be lower than at nominal conditions at any time along the transient.

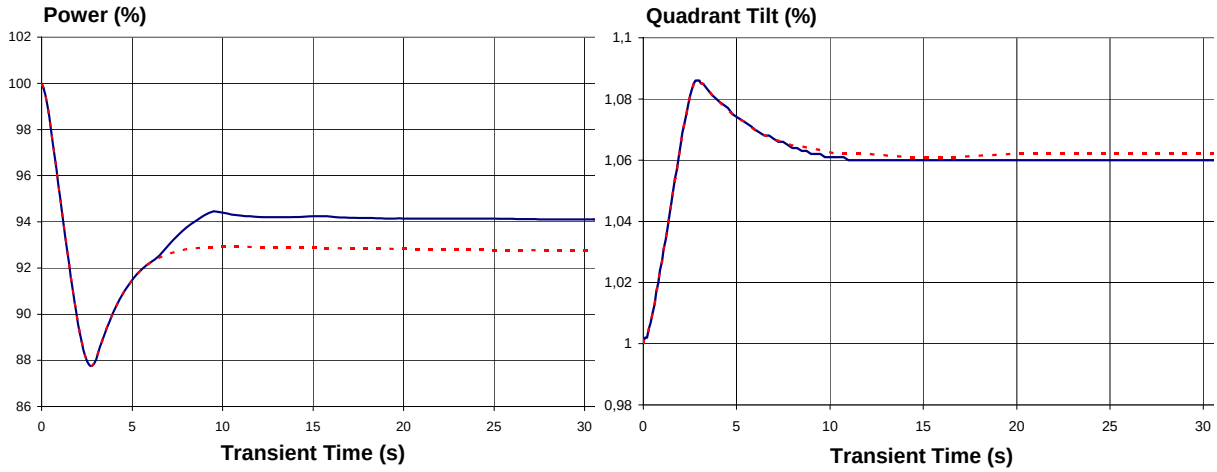

Figure 19. Evolution of nuclear power (left) and quadrant tilt (right) in rod drop transient (broken/solid lines: without/with feedback of core inlet temperatures).

4.2. Phenomenology, measurements and simulation of the control group insertion transient

The chain of events that occurred in this actual transient with fast insertion of a control rod group (4 rods) was:

(1) At 04:26 on 02-dec-2007 a fast insertion (in 12 seconds) of a control rod group (SA1) of 4 rods unexpectedly occurred due to an electronic failure in one instrumentation card for rod motion. Core was near nominal state at 2249 hours (3305 MWd/t) in cycle 16, at 96,2% power (2940 MWt) with bank D inserted at 216 steps and 1212 ppm measured Boron.

(2) The nuclear power dropped quickly to about 65% in 10 seconds, due to the high worth of the 4-rods in the control group. Since the control was in manual mode, because operation was near the end of a routine valve test, the control bank did not react and the turbine continued to demand full steam flow, which caused the secondary steam pressure to drop quickly, while the primary pressure decreased slowly.

(3) At 21 seconds after the initiation of the event the turbine and reactor trip was activated by the low secondary pressure set-point. Almost immediately, the high pressure injection system was also activated and manually closed after 10 minutes after verification of the correct shutdown status, to avoid that the primary became "solid". The plant was brought to cold shutdown status without further incidents.

Figure 20 shows the results of the simulation with SIMTRAN, starting from the online 3D state at the start of the transient, compared with the measurements registered every 0.1 seconds, for the nuclear power level and the axial asymmetry of the excore detectors currents.

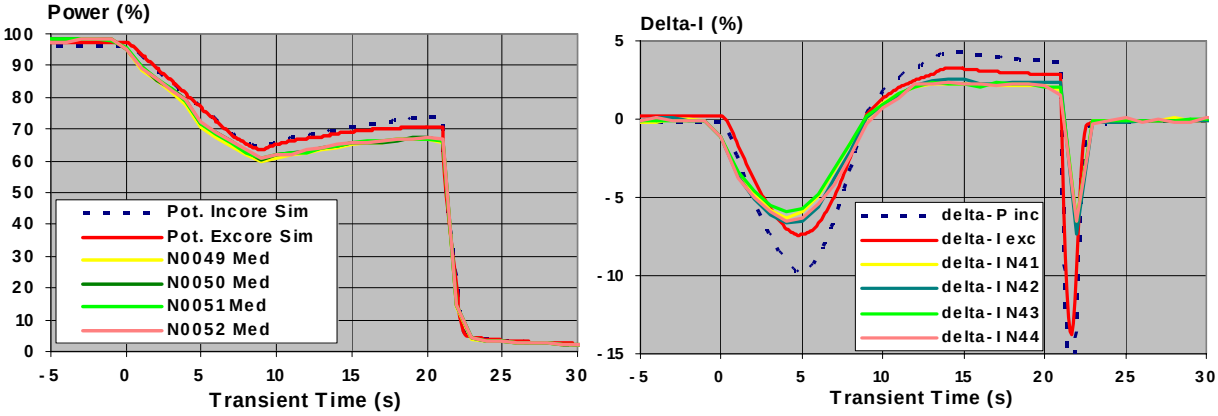

Figure 20. Evolution of nuclear power (left) and axial asymmetry (right) in control group fast insertion transient (broken/solid lines: incore/excore simulation and measurement).

The agreement of the SIMTRAN results for the excore detectors response is quite good, both in their sum (nuclear power level) as in their axial asymmetry (delta-I).

Figure 21 shows the simulated and measured vessel outlet temperatures at the hot legs per loop, also with good agreement taking into account the wider range and time averaging of the measurements.

The safety margins on DNBR and Fq, as well as the maximum fuel and clad temperatures, were also assessed and found to be lower than at initial near-nominal conditions at any time along the transient.

In particular, the Allowed Power Level by Nuclear Design (APLND) was calculated to be above 130% at the initial state, increases to above 180% at the end of the control group fast insertion (at 10 seconds) and then decreases to above 150% at the time of reactor trip, where it increases quite rapidly to much higher levels.

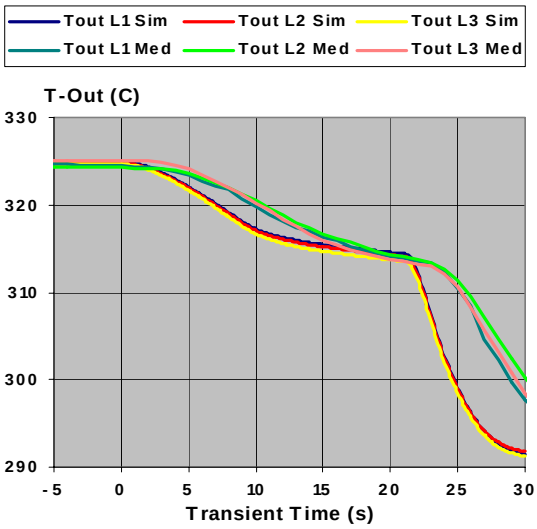

Figure 21. Vessel outlet hot leg temperatures (C) per loop simulated and measured

5. THE NEA/NSC BENCHMARK ON MAIN STEAM LINE BREAK IN PWR

The benchmark on Main Steam Line Break (MSLB) in Pressurized Water Reactors (PWR) was proposed by the Nuclear Science Committee (NSC) of the Nuclear Energy Agency (NEA/OECD). The benchmark is based in the design and operating data of the TMI-1 PWR (B&W) at the end of cycle (EOC0) of a recent 24-months operation cycle, with specifications [19]. It has been carried out from mid-1997 to the end of 2000 [20].

The objectives of this benchmark are [19]:

- Verify the capabilities of the Thermal-Hydraulics system codes to analyze complex transients, with coupled 3-D core neutronics and plant interactions;
- In depth testing of the 3-D neutronics thermal-hydraulics coupling;
- Evaluate the discrepancies between the predictions of the coupled codes in realistic transient conditions.

The phenomenology of the PWR-MSLB transient includes the following main events:

[1] Rupture in guillotine of one main steam line, in 1 of the 2 loops.

[2] Loss of mass, depressurization and increase of the steam flow in the secondary side of the affected steam generator.

[3] Cooling of the primary loop, increase of reactivity and core power and trip.

[4] The most reactive control rod, and closer to the cooled loop, is stuck out of the core.

[5] The continuous cooling (60 s) can result in return to criticality or at least in a return to power (with reduced neutron absorption in control rods).

The *Benchmark* MSLB includes three phases or exercises [19-20]:

1. Plant Simulation, with point-kinetics model for the core and the standard TH modeling of the primary and secondary loops. The objective is to verify the response of the TH system models.
2. Coupled 3-D neutronics and thermal-hydraulics evaluation of the core response. The objective is to verify the 3-D neutronics core response with imposed TH core boundary conditions.
3. Full coupled core-plant *best-estimate* transient modeling. This exercise simulates the full transient combining the two first phases, verifying the coupling of the 3-D core neutron kinetics and the system thermal-hydraulics codes.

5.1 Results of the second exercise PWR-MSLB: steady states and guided transients

The second exercise includes the calculation of 5 steady states, as a help to validate the cross sections and the 3-D core neutronics models. The states 0, 1 and 3 are at zero power, it is with all temperatures and densities uniform in the whole core, and with different insertions of the control rod banks: all rods out (ARO), control bank 7 inserted at 900 steps except rod N12 stuck out of core, and all rods inserted at 0 steps except the same rod N12 stuck out too, respectively. Case 4 is identical to case 3, but with the cross sections for all control rods reduced in their thermal group absorption to allow the hypothetical scenario of return-to-power (rp). Case 2 is at full power and nominal conditions, with control banks as in case 1.

The results obtained with our SIMTRAN code for all of these steady states are given in the following table 1, together with the average values from all the participants in this exercise [20].

Table 1. Results of SIMTRAN and averages of all participants for the steady states

	K-eff		$F_{\Delta H}$		F_Z		A.O. (%)	
Case Code:	Simtran	Average	Simtran	Average	Simtran	Average	Simtran	Average
# 0. HZP, ARO	1.0354	1.0337	1.353	1.361	2.709	2.684	+ 76.5	+ 78.0
# 1. HZP, 90%–N12	1.0335	1.0318	1.443	1.432	2.483	2.452	+ 71.1	+71.7
# 2. HFP, 90%–N12	1.0057	1.0038	1.332	1.350	1.053	1.085	– 0.7	+ 3.8
# 3. HZP, ARI–N12 TRW (3–1)+SRW	0.9884 4.45 %	0.9854 4.53 %	5.916 0.76 %	5.458 0.70 %	2.816	2.754	+ 78.4	+ 79.1
# 4. HZP, ARI–N12 TRW (4–1)+SRW	1.0028 2.99 %	1.0002 3.04 %	3.849 0.43 %	3.630 0.43 %	2.786	2.738	+ 78.1	+ 79.1

Our results, for the steady-states proposed for the exercise 2 of the MSLB Benchmark, show small deviations from the mean results of other participants, especially for core average parameters, as will be fully documented in the final reports of the benchmark [20]. Our detailed 3-D results show higher radial and axial power peaks in the ARI-1 and final states.

In this exercise the transient calculation is limited to the core, in 3-D and coupled N-TH, guided by the Core Boundary Conditions, given along the transient by the TRAC code of the benchmark coordinators. The variables included in the BC are:

- Temperatures at the inlet of the core channels or at the inlet to the vessel of the 2 loops,
- Mass flows at the inlet of the core channels or at the inlet to the vessel per loop,
- Pressure at the lower and upper core plenum (or as core average).

Exercise 2 of the MSLB Benchmark included two guided transients: a Best-Estimate (be) scenario, with the physical control rod absorption XS sets, and a Return-to-Power (rp) scenario, with reduced control rod absorption XS sets. The trip is specified at 0.4 seconds after reaching the 114 % of rated power setpoint. Our results for the "rp" scenario, are given in figure 22, for the evolution of the total core power and the maximum nodal fuel Doppler temperature, together with the results of Purdue/NRC and the mean of all participants [20].

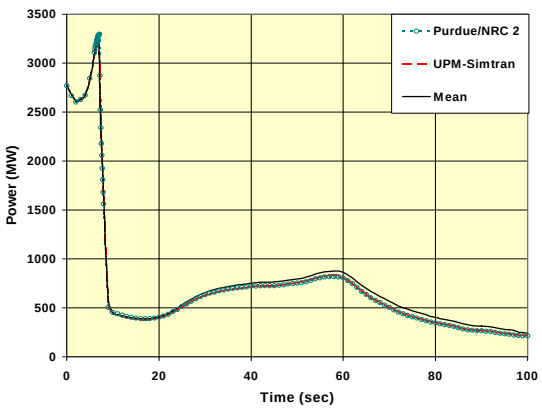

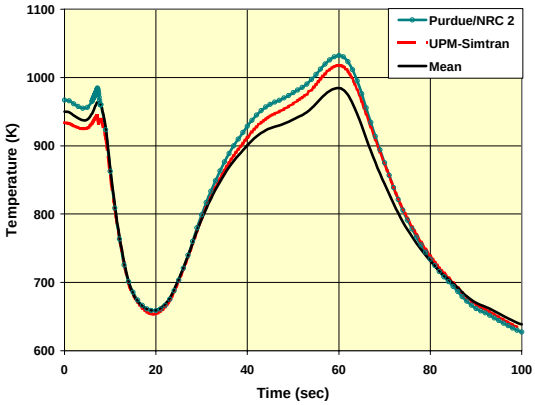

Figure 22. Total core power and maximum nodal temperature versus time in the guided MSLB transient with return to power

In this second exercise the agreement in the evolution of the core power is very good, better than in the first exercise, since the transients have been guided with specified core inlet boundaries conditions. The differences among our SIMTRAN results, using COBRA for core TH, and the Purdue/NRC results using PARCS and RELAP-5, are minimal. In the maximum nodal fuel temperatures (Doppler average) both solutions are in the *cluster* that uses one heat structure (fuel rod) per fuel assembly. For these solutions the maximum fuel temperature is significantly higher at the time of return to power, at 60 seconds, than for other solutions where the heat structures include several fuel assemblies, thus lowering the mean value.

5.2. Results for the third exercise PWR-MSLB: coupled plant and 3-D core transients

We have applied SIMTRAN in its version interfaced with RELAP-5 [12, 15] to the transients of the third exercise of the PWR-MSLB Benchmark, in both scenarios *best-estimate* and *return-to-power*. The neutronics data bases of SIMTRAN are identical to the ones developed and validated in the second exercise. The thermal-hydraulic data bases of RELAP-5 are identical to the ones developed and validated by the Purdue-NRC group in the first and third exercises of the benchmark [21-22], where the whole plant is modeled.

In the following tables 2 to 4 and figures 23 to 25 we collect our results obtained with SIMTRAN coupled to RELAP-5, together with the results obtained by the Purdue-NRC group [21-22] with PARCS coupled to RELAP-5, to verify the agreement of our code implementation.

Table 2 includes the sequence of events and times of occurrence for both MSLB transient scenarios, with both code systems. For both scenarios SIMTRAN/RELAP-5 shows a delay of a few cents of second respect to PARCS/RELAP-5, probably due to the differences in their time coupling, semi-implicit in our case and explicit in the other case.

Table 2. Sequence of events (times in seconds)

Description of event	Best-estimate scenario		*Return-to-power* scenario	
	Simtran+R5	Parcs + R5	Simtran+R5	Parcs + R5
Rupture in main steam line	0.01	0.01	0.01	0.01
Trip of control rods	6.18	6.17	6.18	6.17
Closure of turbine valves	6.68	6.67	6.68	6.67
Injection at high pressure	35.90	35.80	36.03	35.94
Maximum return to power	69.70	68.68	65.83	65.82
End of transient	100.00	100.00	100.00	100.00

The results in the core integral parameters (reactivity or power level) and the power distributions at characteristic times of the transient (radial and axial peaking factors and axial offset of power) also are very close for both code systems. Table 3 includes these parameters at the initial steady state and at the time of

maximum power before the reactor trip, up to the point where both scenarios show the same behavior.

Table 3. Initial steady state at full power and at the time of maximum power before trip

Parameter	Simtran + R5	Parcs + R5
Power at initial state (%)	100	100
Multiplication factor (K-effective)	1.00479	1.00528
Radial assembly power factor (Fxy)	1.326	1.332
Axial core power factor (Fz)	1.062	1.070
Axial Offset of core power (%)	-0.39	+0.47
Power just before trip (%)	118.61	118.12
Radial assembly power factor (Fxy)	1.460	1.464
Axial core power factor (Fz)	1.091	1.072
Axial Offset of core power (%)	-2.72	-1.82

The agreement of both codes is quite good for these safety related parameters, since the differences are well within the acceptance criteria in nuclear design. Table 4, includes the same parameters from the snap-shots at the times of maximum return to power and transient end.

Table 4. Snap-shots at maximum return to power and end of transient

Parameter	*Best-estimate* scenario		*Return-to-power* scenario	
	Simtran+R5	Parcs + R5	Simtran+R5	Parcs + R5
Maximum Power (%)	9.53	9.53	37.09	36.65
Radial Fxy	4.328	4.171	3.693	3.702
Axial Fz	1.927	1.876	1.826	1.847
Axial Offset (%)	+37.25	+35.95	+36.30	+38.0
Final Power (%)	4.74	4.73	8.95	8.64
Radial Fxy	2.161	2.123	2.651	2.737
Axial Fz	1.334	1.317	1.741	1.783
Axial Offset (%)	+11.94	+11.94	+31.54	+34.24

Figure 8 plots the evolution of the dynamical reactivity along the transient as calculated by both code systems for the two scenarios. The *best-estimate* (be) scenario, with realistic cross sections of the control rods, is far from a second criticality with both codes. In the *return-to-power* (rp) scenario, with reduced absorption in the control rod cross sections, we obtain a slight second criticality with the SIMTRAN code.

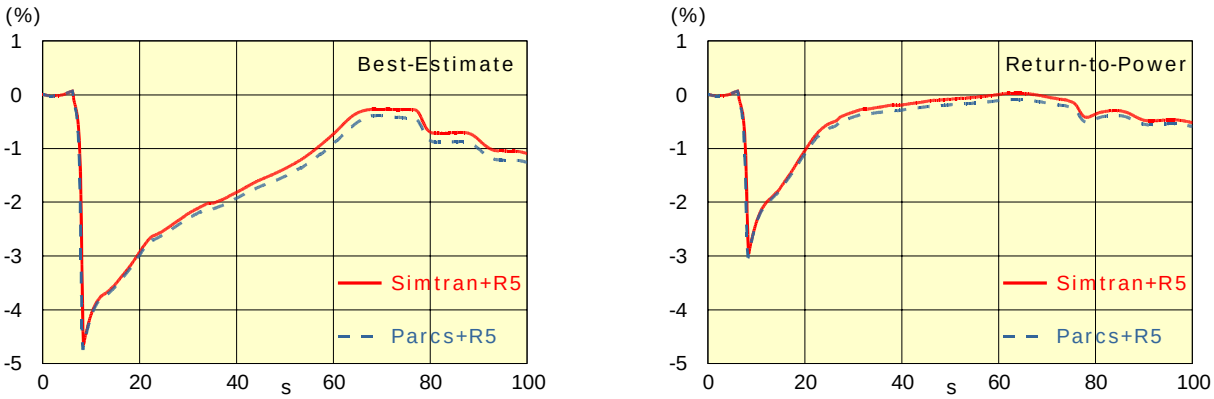

Figure 23. Dynamical reactivity evolution with SIMTRAN+RELAP5 and PARCS+RELAP5

Figure 24 plots the evolution along the transients of the total core power for both code systems, with a very good agreement, and the core fission power calculated by SIMTRAN, where the residual decay heat is

calculated following the benchmark specifications: the initial 3-D shape as a fraction of the total power is modulated afterwards by the total decay heat given in tables for both scenarios.

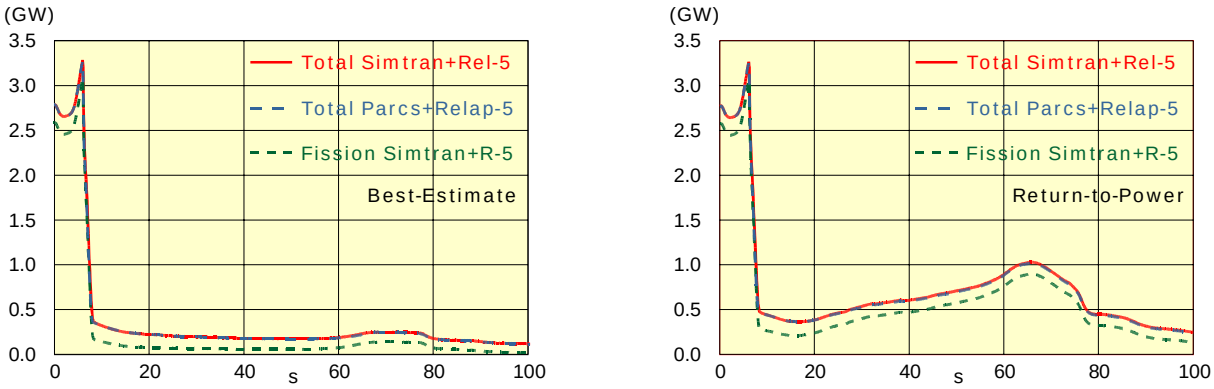

Figure 24. Core Total and Fission Powers with SIMTRAN+RELAP5 and PARCS+RELAP5

The agreement in the maximum nodal fuel temperatures (Doppler) is very good for the return-to-power (rp) case, as in the core average Doppler temperature for both scenarios. In the best-estimate (be) case a slightly higher difference is observed at the second maximum.

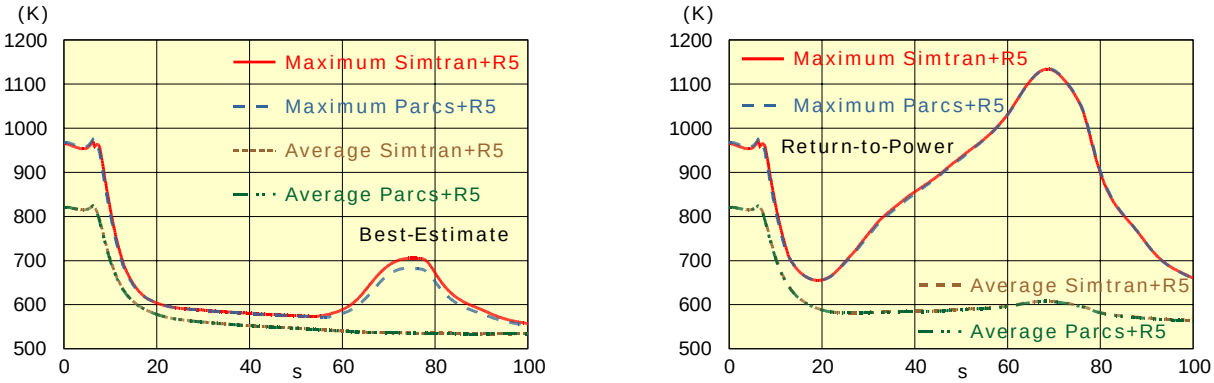

Figure 25. Core average and maximum nodal fuel temperatures in MSLB transients with SIMTRAN+RELAP5 and PARCS+RELAP5

We remark the increase in about 20 % of the maximum fuel temperature, respect to the initial, that is obtained using one mean fuel rod as heat structure in RELAP per fuel assembly, and the remarkable agreement between both codes at that maximum fuel temperature (rp case).

We conclude that we have successfully validated our SIMTRAN code for both core transient analysis and for whole system transient analysis, coupled to RELAP-5 or other TH system code.

6. Current issues and ongoing developments

The coupled 3-D neutron kinetics and thermal hydraulics computation is a state-of-the-art issue for best-estimate design and safety analysis of present and advanced LWRs and other reactor types. Several code systems have been implemented and validated, ie with the NEA-NSC LWR transient benchmarks, in the last years.

But these codes model the whole LWR cores by coarse-mesh neutronics nodes and TH channels, with the size of full or quarter fuel assemblies, without detailed solutions and feedbacks at the fuel pin or subchannel level [16-18], which are required to asses the local thermal and mechanical design and safety limits.

This is the ongoing R+D work of the NURESIM integrated project [23-28], being completed under Euratom FP6, and its continuation cooperative project NURISP, just proposed to Euratom FP7.

References

1. F. Merino, C. Ahnert, J.M. Aragonés, *"Development and Validation of the 3-D PWR Core Dynamics SIMTRAN Code"*, in Mathematical Methods and Supercomputing in Nuclear Applications, H. Kusters (Ed.), Vol. 1, 646-657, ANS-KfK, Karlsruhe, (1993).
2. J.M. Aragonés, C. Ahnert, "*Computational Methods and Implementation of the 3-D PWR Core Dynamics SIMTRAN Code for Online Surveillance and Prediction*", in Mathematics and Computation, Reactor Physics and Environmental Analysis, L. Briggs (Ed.), Vol. 1, 237, American Nuc. Soc., Portland (1995).
3. J.M. Aragonés, C. Ahnert, O. Cabellos, "*Methods and Performance of the 3-D PWR Core Dynamics SIMTRAN Online Code*", Nucl. Sci. Eng. **124(1)**, 111-124 (1996).
4. O. Cabellos, C. Ahnert, J.M. Aragonés, "*Generalized Effects in Two-Group Cross Sections and Discontinuity Factors for PWR's*", Proceedings of the International Conference on the Physics of Reactors (PHYSOR 96), Mito, Ibaraki (Japón), Vol. 1, B-82-91 (1996).
5. J.M. Aragonés, C. Ahnert, D. Cano, N. García-Herranz, "*Planing of Operational Maneuvers with the 3-D PWR Core Dynamics SIMTRAN Online code*", Proceedings of the International Conference on the Physics of Reactors (PHYSOR 96), Mito, Ibaraki (Japón), Vol. 4, K-9-17 (1996).
6. J.M. Aragonés, C. Ahnert, V. Aragonés-Ahnert, *"Coupled 3-D Neutronic-Thermalhydraulic Analysis of Transients in PWR Cores"*, in Mathematical Methods and Supercomputing for Nuclear Applications, F. Brown (Ed.), Vol. 2, 1380-1390, American Nuclear Soc., Saratoga (1997).
7. J.W. Jackson, N.E. Todreas, "*COBRA IIIc/MIT-2: A Computer Program for Steady State and Transient Thermo-Hydraulic Analysis of Rod Bundle Nuclear Fuel Elements*", MIT report, Boston (1981).
8. C. Ahnert, J.M. Aragonés, O. Cabellos, N. García-Herránz, "*Continuous Validation and Development for Extended Applications of the SEANAP Integrated 3-D PWR Core Analysis System*", in Mathematics and Computation, Reactor Physics and Environmental Analysis in Nuclear Applications, J.M. Aragonés (Ed.), Vol. 1, 710-719, Senda Ed., Madrid (1999).
9. N. García-Herranz, J.M. Aragonés, O. Cabellos, C. Ahnert, "*Dependence of the Nodal Homogenized Two-Group Cross Sections on Intranodal Flux-Spectrum, Burnup and History*", in Mathematics and Computation, Reactor Physics and Environmental Analysis in Nuclear Applications, J.M. Aragonés (Ed.), Vol. 1, 127-138, Senda Ed., Madrid (1999).
10. O. Cabellos, J.M. Aragonés, C. Ahnert, "*Generalized Effects in Two Group Cross Sections and Discontinuity Factors in the DELFOS Code for PWR Cores*", in Mathematics and Computation, Reactor Physics and Environmental Analysis in Nuclear Applications, J.M. Aragonés (Ed.), Vol. 1, 700-709, Senda Ed., Madrid, (1999).
11. J.M. Aragonés, "*Coupled 3-D Neutronic and Thermal-Hydraulic Transient Calculations for Deterministic Safety Analysis*", Frederic-Joliot–Otto-Hahn Summer School on Reactor Physics, CEA, Cadarache (2000).
12. J.M. Aragonés, C. Ahnert, O. Cabellos, N. García-Herranz, V. Aragonés-Ahnert, "*Methods and Results for the MSLB NEA Benchmark using SIMTRAN and RELAP-5*", Trans. Am. Nuc. Soc. **84**, 23, Milwaukee (2001).
13. N. García-Herranz, O. Cabellos, J.M. Aragonés, C. Ahnert, "*Performance of the Analytic Coarse Mesh Finite Difference Method with Heterogeneous Nodes*", Physor-2002, International Reactor Physics Conference, Seoul (2002).
14. N. García-Herranz, O. Cabellos, J.M. Aragonés, C. Ahnert, "*Analytic Coarse Mesh Finite Difference Method Generalized for Heterogeneous Multidimensional Two-Group Diffusion Calculations*", Nucl. Sci. Eng. **144**, 23-35 (2003).
15. J.M. Aragonés, C. Ahnert, O. Cabellos, N. García-Herranz, V. Aragonés-Ahnert, "*Methods and Results for the MSLB NEA Benchmark using SIMTRAN and RELAP-5*", Nuclear Technology **146**, 29-40 (2004).
16. D. Cuervo, M.N. Avramova, K.N. Ivanov, "*Improving the Computation Efficiency of COBRA-TF for LWR Safety Analysis of Large Problems*", in PHYSOR 2004 -The Physics of Fuel Cycles and Advanced Nuclear Systems: Global Developments, Paper 6B, 95464, American Nuclear Society, Chicago (2004).
17. D. Cuervo, C. Ahnert, J.M. Aragonés, "*Analysis of Subchannel Effects and their Treatment in Average Channel PWR Core Models*", The 6th International Conference on Nuclear Thermal Hydraulics,

Operations and Safety (NUTHOS-6), Paper ID. N6P215, Nara, Japan (2004).

18. D. Cuervo, C. Ahnert, J.M. Aragonés, "*Analysis of the Influence of Subchannel Effects on the PWR Average Channel Calculations*", in 11th International Topical Meeting on Nuclear Reactor Thermal Hydraulics (NURETH-11), Hervé Lemmonnier Ed., Paper ID. D5-P396, American Nuclear Society, Avignon, France, 2-6 Octubre (2005).
19. K.N. Ivanov, T.M. Beam, A. Baratta and A. Irani, *"Pressurized Water Reactor Main Steam Line Break (MSLB) Benchmark, Vol. I: Final Specifications*". NEA/NSC/DOC(97)15, US-NRC/OECD-NEA, París (1997).
20. K.N. Ivanov, T.M. Beam, A. Baratta and A. Irani, *"Pressurized Water Reactor Main Steam Line Break (MSLB) Benchmark, Vol. II: Summary Results of Phase I (Point Kinetics)*". NEA/NSC/DOC (00) 20, US-NRC/OECD-NEA, París (2000).
21. D. Barber et al., *"Coupled 3-D Reactor Kinetics and Thermal-Hydraulic Code Activities at the US-NRC"*, in Mathematics and Computation, Reactor Physics and Environmental Analysis in Nuclear Applications, J.M. Aragonés (Ed.), Vol 1, 311-320, Senda Ed., Madrid (1999).
22. R. Miller et al., *"Analysis of the OECD MSLB Benchmark with RELAP-PARCS and TRAC-M-PARCS"*, in Mathematics and Computation, Reactor Physics and Environmental Analysis in Nuclear Applications, J.M. Aragonés (Ed.), Vol 1, 321-332, Senda Ed., Madrid (1999).
23. J.M. Aragonés, C. Ahnert, N. García-Herranz, "The Analytic Coarse-Mesh Finite Difference Method for Multigroup and Multidimensional Diffusion Calculations", Nucl. Sci. Eng. 157, 1-15 (2007).
24. J.A. Lozano, J.M. Aragonés, N. García-Herranz, "Development and Performance of the Analytic Nodal Diffusion Solver ANDES in Multigroups for 3D Rectangular Geometry", in Mathematics & Computations and Supercomputing in Nuclear Applications, M&C/SNA-2007 Monterey CA, T. Rubia, J. Vujic (Eds.), Vol. 4A5, 1-13, American Nuclear Society Ed., La Grange Park, IL-USA, ISBN: 0-89448-059-6 (2007).
25. J.J. Herrero, C. Ahnert, J.M. Aragonés, "3D Whole Core Fine Mesh Multigroup Diffusion Calculations by Domain Decomposition through Alternate Dissections", in Mathematics & Computations and Supercomputing in Nuclear Applications, M&C/SNA-2007 Monterey CA, T. Rubia, J. Vujic (Eds.), Vol. 8D9, 1-13, American Nuclear Society Ed., La Grange Park, IL-USA, ISBN: 0-89448-059-6 (2007).
26. J. Jiménez, D. Cuervo, J.M. Aragonés, "Multiscale and Multiphysics Coupling in COBAYA3", in Nuclear Reactor Thermal-hydraulics, NURETH-12 Pittsburgh PA, 12 pp., Am. Nuc. Soc. Ed., La Grange Park, IL-USA, ISBN: (2007). Selected for publication in Nucl. Eng. and Design.
27. D. Cacuci, J.M. Aragonés, D. Bestion, P. Coddington, L. Dada, and C. Chauliac, "*NURESIM: A European Platform for Nuclear Reactor Simulation*", invited paper in FISA 2006 - EU Research and Training in Reactor Systems - EUR 21231, pp. 123-143, European Commission DG for Research Euratom, Luxembourg, ISBN: 92-79-01214-2 (2006).
28. J.M. Aragonés, "*Qualification of Core Physics Codes within NURESIM*", in Post-FISA Seminar on Qualification of Advanced Numerical Simulation Platforms, FISA 2006 - EU Research and Training in Reactor Systems - EUR 21231, pp. 572-588, European Commission DG for Research Euratom, Luxembourg, ISBN: 92-79-01214-2 (2006).